

BIFURCATION THEORY APPLIED TO THE ANALYSIS OF POWER SYSTEMS

GUSTAVO REVEL, DIEGO M. ALONSO, AND JORGE L. MOIOLA

ABSTRACT. In this paper, several nonlinear phenomena found in the study of power system networks are described in the context of bifurcation theory. Toward this end, a widely studied 3-bus power system model is considered. The mechanisms leading to static and dynamic bifurcations of equilibria as well as a cascade of period doubling bifurcations of periodic orbits are investigated. It is shown that the cascade verifies the Feigenbaum's universal theory. Finally, a two parameter bifurcation analysis reveals the presence of a Bogdanov-Takens codimension-two bifurcation acting as an organizing center for the dynamics. In addition, evidence on the existence of a complex global phenomena involving homoclinic orbits and a period doubling cascade is included.

1. INTRODUCTION

Power systems *blackouts* have received a great attention in the last few years, due to the increasing amount of incidents occurred in many countries around the world (see for example [17, 20, 3, 27] and references therein). For different reasons many systems are forced to operate near to their stability limits and thus they are vulnerable to perturbations of the operating conditions. When these limits are exceeded, the system can exhibit undesired transient responses with the impossibility to retain a stable voltage profile. This phenomenon is known as voltage collapse. Factors that influence it are increments in the load consumption that reach the limits of the network or the generation capacity, actions of badly tuned controllers, tripping of lines and generators, among others [6].

Power system networks are one of the more complex and difficult systems to model. The first problem is the size, just imagine a large-scale network composed by hundreds of generators connected by thousands of transmission lines and buses, along with probably hundreds of load centers, as it is easy to find in almost every country. A second problem is its complex nature. Physical variables with very different time scales (the electrical variables are sometimes extremely faster than the mechanical states of the generators), devices modelled by continuous dynamics (generators, loads, etc.) combined with discrete events (faults, controllers, etc.),

Key words and phrases. nonlinear systems, power systems, voltage collapse, numerical analysis, bifurcations, chaos.

This work was partially supported by UNS (PGI 24/K041), CONICET (PIP5032) and ANPCyT (PICT-06-00828).

algebraic restrictions (network constraints, operating conditions, etc), are some of the main features revealing the complexity of the system. Therefore, to deal with a tractable model it is necessary to make simplifications such as replacing a group of generators, lines and/or loads for a single device with an equivalent behavior, or neglecting fast dynamics, etc. By far, the usual approach to model a power system is using a differential-algebraic set of equations (DAE model) of the form [13, 23]

$$\begin{aligned}\dot{x} &= f(x, y; \lambda), \\ 0 &= g(x, y; \lambda),\end{aligned}$$

where $f : R^{n \times m \times p} \rightarrow R^n$, $g : R^{n \times m \times p} \rightarrow R^m$, $x \in R^n$ represents the differential or dynamical state variables, $y \in R^m$ represents the algebraic state variables, and $\lambda \in R^p$ is a vector of real parameters. The differential variables include the mechanical states of the generators (swing equations), the electrical states of the rotor, the excitation and governor systems (voltage and frequency controls, respectively) and the dynamical states of the load. On the other hand, the algebraic states are mainly determined by the transmission network and algebraic states of the generators stators and loads*. It is easy to obtain a high dimensional DAE model from a real power system. For example, a widely studied system corresponding to the Western System Coordinating Council (WSCC) composed by three machines and nine buses [2, 19, 23], is modelled with 45 equations, 21 differential and 24 algebraic. The total number of equations might vary according to the detail used when modelling generators and loads. A more complete model results from considering an hybrid system which is described by a set of differential-algebraic-difference (DAD) equations [11], to accurately include faults and the discrete nature of some components of the system. Nevertheless, it is important to notice that the complexity of the model depends on the problem under study.

In addition, power systems are highly nonlinear and its dynamical behavior may change qualitatively when parameters are varied. For example, after a load increment a stable operating point may become unstable and oscillations arise. This behavior can be locally associated to a Hopf bifurcation and, in general, bifurcation theory can be applied to understand mechanisms leading to nonlinear phenomena in these systems. The idea underlying a bifurcation analysis is to investigate qualitative changes in the system dynamics (e.g. stability loss, birth or death of oscillations, passage from periodic to chaotic solutions or viceversa, etc.) under *slow* variations of distinctive system parameters. In this regard, [1] and [15] present results in the study of steady state stability of power systems considering dynamic (Hopf) and static (saddle-node) bifurcations, respectively. Then, Dobson and Chiang [5] have introduced a simple 3-bus power system model showing that the interaction between the load and generator causes a saddle-node bifurcation. As

*The algebraic states arise from neglecting the dynamics of lines (instantaneous power transference) and other devices. Although it is unusual, specially for large systems, the fast dynamics can be included and thus the system can be modelled by a set of ordinary-differential equations (ODE) [22]. In refined studies, the differential equations representing the transmission lines can be replaced by a set of partial-differential equations (PDE), since the impedance is distributed along the line [12].

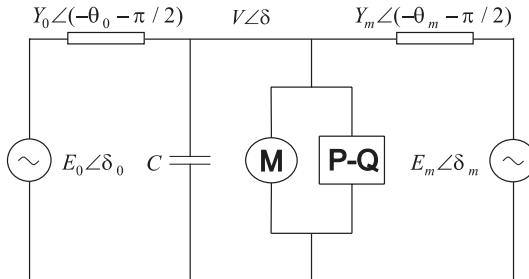


FIGURE 1. Schematic diagram of the 3-bus electric power system model.

a consequence the stable operating point disappears if the reactive power demand is increased and then the voltage on the load suddenly drops to zero (voltage collapse). This simple model has been widely studied using different sets of parameter values (e.g. [29, 26, 16, 4]). For example, Wang et al. [29] have shown that this system can develop a voltage collapse following a cascade of period doubling bifurcations. Later, Budd and Wilson [4] have found a Bogdanov-Takens bifurcation point when considering two parameter variations.

In this paper, the 3-bus power system model is revisited. An overview of bifurcations when varying one and two parameters is presented. It is shown that in a one parameter bifurcation analysis, saddle-node and Hopf bifurcations of equilibria are the mechanisms by means an operating point can disappear or become unstable, respectively. In addition, the periodic orbit born at the Hopf bifurcation undergoes a cascade of period doubling bifurcations leading to a chaotic attractor. It is shown that the cascade follows the theory proposed by Feigenbaum [8, 9]. When considering variations of two parameters, a Bogdanov-Takens codimension two bifurcation point is detected for positive values of the active and reactive power of the load. Even though the unfolding of this bifurcation seems not to affect *a priori* the operating point of the system, the appearance of additional global phenomena can influence the behavior over regions of practical importance.

This paper is organized as follows. In section 2 the model of the power system is described. One and two parameter bifurcation analysis are developed in sections 3 and 4, respectively. Finally, in section 5 some concluding remarks are presented.

2. MATHEMATICAL MODEL OF A 3-BUS ELECTRIC POWER SYSTEM

The 3-bus power system model introduced in [5] and shown in Fig. 1, consists of an infinite bus on the left, a load bus on the center and a generator bus on the right. $Y_0\angle(-\theta_0 - \pi/2)$ and $Y_m\angle(-\theta_m - \pi/2)$ are the admittances of the transmission lines.

The concept of an infinite bus refers to a particular node of the system with enough capacity to absorb any mismatch in the power balance equations. Thus, it can be considered as a fictitious generator with constant voltage magnitude E_0 and phase δ_0 (usually $E_0 = 1$ and $\delta_0 = 0$). This approach is valid specially when working with a small subsystem connected to a large-scale power grid. On the

other hand, the generator has constant voltage magnitude E_m but the angle δ_m varies according to the so-called swing equation

$$M\ddot{\delta}_m + d_m\dot{\delta}_m = P_m - P_e, \quad (2.1)$$

where M is the inertia of the rotor, d_m is the damping coefficient, P_m is the mechanical power supplied to the generator and P_e is the electric power supplied by the generator to the network (including the loss in Y_m) given by

$$P_e = -E_m Y_m [E_m \sin(\theta_m) + V \sin(\delta - \delta_m + \theta_m)]. \quad (2.2)$$

Replacing (2.2) in (2.1), the dynamics of the generator is reproduced by the *classical* model of a voltage generator (also known as *constant voltage behind reactance* [24])

$$\dot{\delta}_m = \omega \quad (2.3)$$

$$\dot{\omega} = \frac{1}{M} [-d_m \omega + P_m + E_m^2 Y_m \sin(\theta_m) + E_m V Y_m \sin(\delta - \delta_m + \theta_m)]. \quad (2.4)$$

The load bus, with voltage magnitude V and phase δ , consists of an induction motor, a generic load P-Q and a capacitor C . The dynamics of this part is derived from a power balance at the bus. Considering an empirical model for the induction motor [28] and a static load P-Q, the power consumption results

$$\begin{aligned} P_{load} &= \underbrace{P_0 + k_{pw}\dot{\delta} + k_{pv}(V + T\dot{V})}_{P_{motor}} + P_1, \\ Q_{load} &= \underbrace{Q_0 + k_{qw}\dot{\delta} + k_{qv}V + k_{qv_2}V^2}_{Q_{motor}} + Q_1, \end{aligned}$$

where T , k_{pw} , k_{pv} , k_{qw} , k_{qv} and k_{qv_2} are constants of the motor, P_0 , Q_0 and P_1 , Q_1 are the static active and reactive power drained by the motor and by the load P-Q, respectively. In terms of bus voltages and lines admittances, the active and reactive power supplied to the load are

$$\begin{aligned} P(\delta_m, \delta, V) &= -E'_0 Y'_0 V \sin(\delta + \theta'_0) - E_m Y_m V \sin(\delta - \delta_m + \theta_m) \\ &\quad + V^2 [Y'_0 \sin(\theta'_0) + Y_m \sin(\theta_m)], \end{aligned} \quad (2.5)$$

$$\begin{aligned} Q(\delta_m, \delta, V) &= E'_0 Y'_0 V \cos(\delta + \theta'_0) + E_m Y_m V \cos(\delta - \delta_m + \theta_m) \\ &\quad - V^2 [Y'_0 \cos(\theta'_0) + Y_m \cos(\theta_m)], \end{aligned} \quad (2.6)$$

where E'_0 , Y'_0 and θ'_0 are obtained from a Thevenin equivalent of the circuit towards the infinite bus including the capacitor C , and their expressions are

$$E'_0 = \frac{E_0}{\Gamma}, \quad Y'_0 = Y_0 \Gamma, \quad \theta'_0 = \theta_0 + \tan^{-1} \left(\frac{CY_0^{-1} \sin(\theta_0)}{1 - CY_0^{-1} \cos(\theta_0)} \right),$$

$$\text{with } \Gamma = \sqrt{1 + C^2 Y_0^{-2} - 2CY_0^{-1} \cos(\theta_0)}.$$

Then the balance between the supplied power (P, Q) and the drained power (P_{load}, Q_{load}) at the load bus results in

$$P(\delta_m, \delta, V) = P_0 + k_{pw}\dot{\delta} + k_{pv}(V + T\dot{V}) + P_1, \quad (2.7)$$

$$Q(\delta_m, \delta, V) = Q_0 + k_{qw}\dot{\delta} + k_{qv}V + k_{qv_2}V^2 + Q_1. \quad (2.8)$$

From (2.8)

$$\dot{\delta} = \frac{1}{k_{qw}} [-k_{qv_2}V^2 - k_{qv}V - Q_0 - Q_1 + Q(\delta_m, \delta, V)]. \quad (2.9)$$

Substituting (2.9) into (2.7) and solving for \dot{V} , results

$$\begin{aligned} \dot{V} = & \frac{1}{Tk_{qw}k_{pv}} \{ k_{pw}k_{qv_2}V^2 + (k_{pw}k_{qv} - k_{qw}k_{pv})V \\ & + k_{qw}[P(\delta_m, \delta, V) - P_0 - P_1] - k_{pw}[Q(\delta_m, \delta, V) - Q_0 - Q_1] \}. \end{aligned} \quad (2.10)$$

Equations (2.3–2.4) and (2.9–2.10) with $P(\cdot)$ and $Q(\cdot)$ given by (2.5) and (2.6), respectively, describe the dynamics of the 3-bus system model in terms of the state variables δ_m , ω , δ , and V . The free parameters used in the bifurcation analysis are Q_1 and P_1 , i.e. the reactive and active power drained by the static P-Q load. Therefore the model has the form

$$\dot{x} = f(x, \lambda) \quad (2.11)$$

where $x = [\delta_m, \omega, \delta, V]^T$ is the state vector and $\lambda = [Q_1, P_1]^T$ is the parameter vector. The values of the fixed parameters used in the following numerical study are obtained from [29]: $M = 0.01464$, $C = 3.5$, $E_m = 1.05$, $Y_0 = 3.33$, $\theta_0 = \theta_m = 0$, $k_{pw} = 0.4$, $k_{pv} = 0.3$, $k_{qw} = -0.03$, $k_{qv} = -2.8$, $k_{qv_2} = 2.1$, $T = 8.5$, $P_0 = 0.6$, $Q_0 = 1.3$, $E_0 = 1$, $Y_m = 5.0$, $P_m = 1.0$ and $d_m = 0.05$. All the constants are normalized according to a given basis (“per-unit” representation), except for the angles which are given in degrees.

3. ONE PARAMETER BIFURCATION ANALYSIS

Let us denote the 3-bus power system operation point as $x^* = [\delta_m^*, \omega^*, \delta^*, V^*]^T$, which is normally a stable equilibrium of (2.11) for some λ , i.e. $f(x^*, \lambda) = 0$. The location of x^* changes as the parameter vector λ varies. In addition, the qualitative dynamical behavior in the neighborhood of x^* , may change at particular values of λ , say $\lambda = \lambda^*$. At these points, system (2.11) undergoes local bifurcations and the Jacobian matrix

$$J = \frac{\partial f}{\partial x}(x^*, \lambda^*) \quad (3.1)$$

becomes singular. Considering variations of only one parameter and assuming that some nondegeneracy conditions hold, the equilibrium point x^* exhibits a codimension-one bifurcation when a single eigenvalue of (3.1) crosses the imaginary axis at the origin or when a pair of eigenvalues cross it with nonzero imaginary part. In the first case, one of the associated mechanisms is the saddle-node bifurcation, where the equilibrium point (stable) disappears by coalescing with another equilibrium point (unstable). In the second case, the mechanism is associated to a Hopf

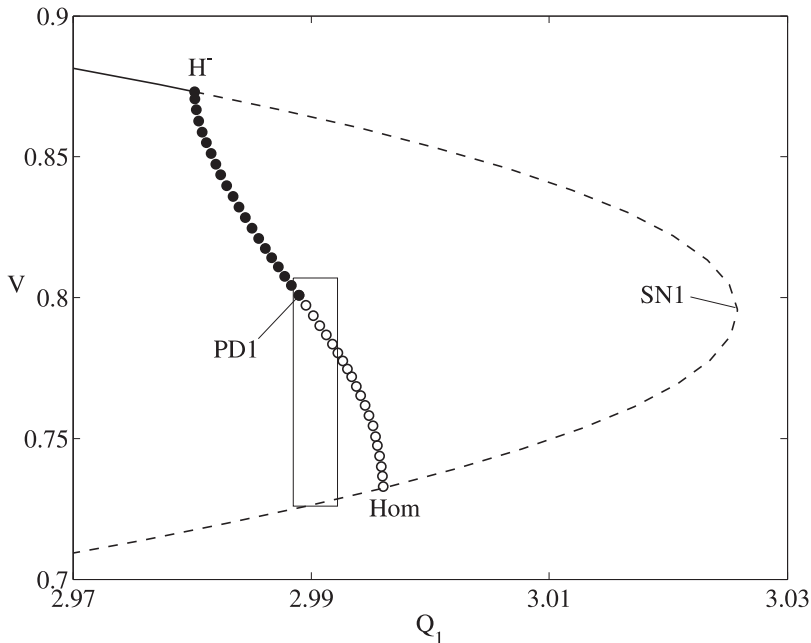


FIGURE 2. Bifurcation diagram varying Q_1 with $P_1 = 0$.

bifurcation. The equilibrium changes the stability and a limit cycle (oscillation) is created in its neighborhood. Further details on the analysis of different bifurcations can be seen, for example in [10] and [14].

In the following one parameter bifurcation analysis, the load reactive power Q_1 is the free parameter while the active power is fixed at $P_1 = 0$. The analysis is performed numerically with the continuation package AUTO [7]. In this setting the equilibrium curve is computed as the main bifurcation parameter is varied and, simultaneously, bifurcation conditions are checked. Figure 2 shows the resulting bifurcation diagram. The curve is denoted as a solid line when the equilibrium is stable and dashed when it is unstable. The value of the state variable V at equilibrium is shown in the ordinate axis. In addition, the minimum value of the amplitude of the periodic orbit born at the Hopf bifurcation is plotted. Filled circles mean stable periodic orbits and empty circles denote unstable ones.

Beginning from the left in Fig. 2, there are two equilibrium points, one stable (where the system may operate) and the other unstable. The stable one becomes unstable at a supercritical Hopf bifurcation (H^-) for $Q_1 = 2.9802182780$ leading to the appearance of a stable limit cycle. For increasing values of Q_1 , both equilibria approach each other and coalesce in a saddle-node bifurcation ($SN1$) for $Q_1 = 3.0257810109$. If the reactive power of the load Q_1 is increased beyond this value, the system does not have an operating point, and voltage collapse occurs.

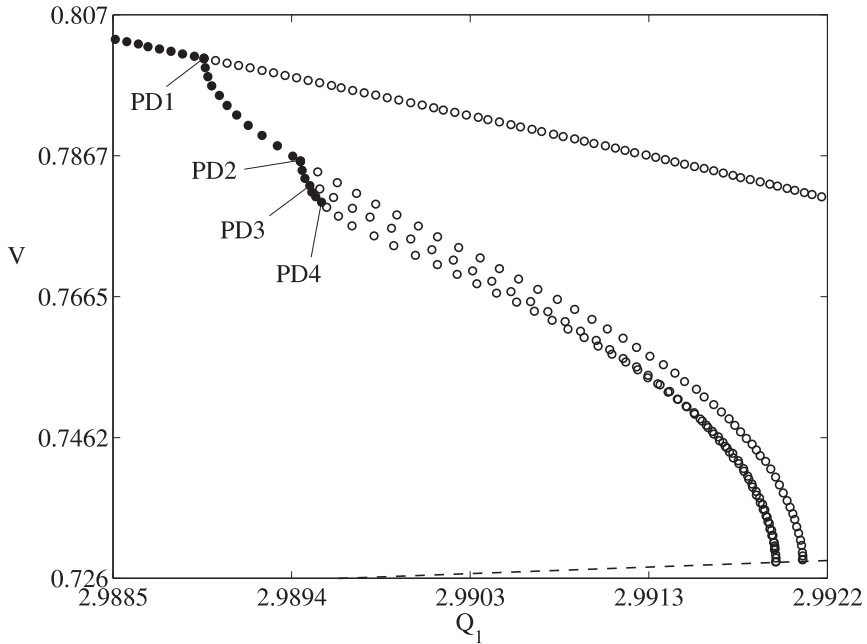


FIGURE 3. Detailed view of the sequence of period doubling bifurcations.

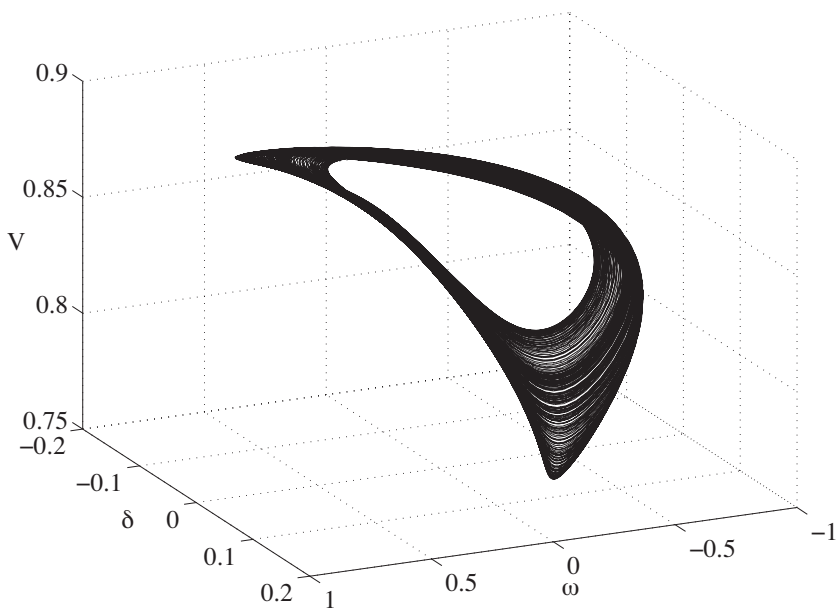
Nevertheless, voltage collapse may be found below this point due to a more complex phenomenon [29] described next.

The cycle born at the Hopf bifurcation (H^-) undergoes a cascade of period doubling bifurcations, i.e. the period of the orbit is doubled repeatedly. This singularity can not be detected from a local analysis around the equilibrium point. Nevertheless, local bifurcations of limit cycles can be detected analyzing the eigenvalues of the associated Poincaré map. When a single eigenvalue crosses the unit circle through 1 or -1 , a saddle-node or a period doubling bifurcation of limit cycles arises, respectively. When a pair of eigenvalues cross the unit circle at $e^{\pm j2\pi/k}$ with $k \neq 0, 1, \dots, 4$ [†], the cycle evidences a Neimark-Sacker or secondary Hopf bifurcation, leading to quasiperiodic motions. In the 3-bus power system under study, the first period doubling bifurcation (PD1) occurs at $Q_1 = 2.9889650564$. At this point, a stable period-two cycle is created, coexisting with the original period-one cycle, now unstable. This cycle becomes unstable at PD2 and a period-four cycle arises. The beginning of the cascade is shown in Fig. 3 which is the blow-up of the rectangle of Fig. 2 (the corresponding values of Q_1 can be obtained from Table 1). This process continues for increasing values of Q_1 and leads to a chaotic attractor. A projection of this attractor for $Q_1 = 2.989790$ is depicted in Fig. 4.

[†]This condition avoids more complex scenarios known as *strong resonances* (see, for example [14], for details on this topic).

TABLE 1. Period doubling bifurcations.

Bifurcation	Q_1
PD1	2.9889650564
PD2	2.9894727221
PD3	2.9895623607
PD4	2.9895809828
PD5	2.9895849451
PD6	2.9895857918
PD7	2.9895859732

FIGURE 4. Chaotic attractor for $Q_1 = 2.989790$.

The attractor, and the associated unstable orbits, collide with the saddle equilibrium point for $Q_1 \simeq 2.996$ and they are destroyed due to boundary crisis bifurcations. Therefore when the chaotic attractor coalesces, the system does not have any stable attractor and the voltage collapse occurs, more precisely after a long chaotic transient the voltage drops to zero suddenly.

3.1. Analysis of the period doubling route to chaos. For unimodal maps, the values of the parameter where the period doubling bifurcations occur are related by a universal constant due to M. J. Feigenbaum [8, 9] given by:

$$\delta_F = \lim_{n \rightarrow \infty} \frac{r_{n+1} - r_n}{r_{n+2} - r_{n+1}} = 4.6692016091\ldots, \quad (3.2)$$

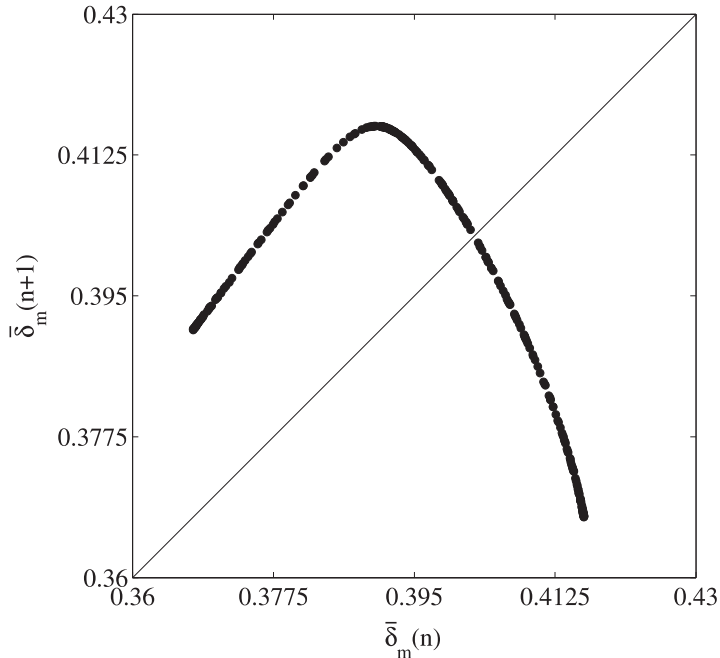


FIGURE 5. Unimodal Lorenz's map for $\bar{\delta}_m$.

where r_j are the parameter values corresponding to the period doubling bifurcations. These results may be approximately applied to ordinary differential equations if the associated Lorenz's map is unimodal [25].

Extending this idea to the power system model, the Lorenz's map is obtained numerically by plotting the successive local maxima of the state variable δ_m when the system is in chaotic regime. The plot, shown in Fig. 5, is very close to a one dimensional curve and can be approximated by an unimodal map. Then, successive approximations to Feigenbaum's universal constant (for n finite) can be computed using

$$\delta_{Fn} = \frac{r_{n+1} - r_n}{r_{n+2} - r_{n+1}}$$

and the values of Q_1 given in Table 1. The resulting approximations are given in Table 2. Notice that the estimation approaches $\delta_F = 4.6692016091\dots$ as n is increased. Thus, knowing the values of Q_1 for the first period doubling bifurcations (i.e. PD1, PD2, PD3, etc.) the occurrence of the remaining bifurcation points can be approximately predicted using δ_F . For example, PD8 can be predicted using δ_F , PD6 and PD7 from Table 1, the result is $PD8 \simeq 2.9895860121$. Although from a practical point of view this is not important, the parameter value corresponding to the chaotic regime can be obtained approximately by applying recursively the relationship, resulting $Q_1 \simeq 2.9898860226$.

TABLE 2. Approximated values of Feigenbaum's universal constant.

n	δ_{Fn}
1	5.663471986396961
2	4.813560232131420
3	4.699820811612138
4	4.679697647450078
5	4.667585450683690

4. TWO PARAMETER BIFURCATION ANALYSIS

Suppose that an equilibrium point or a limit cycle of system (2.11) undergoes a bifurcation for $\lambda = \lambda^*$ when variations of one parameter are considered. Then, varying a second parameter simultaneously, there exists a curve in the parameter plane along which this bifurcation persists. At isolated points on this curve of codimension-one bifurcations, system (2.11) can exhibit codimension-two bifurcations. This situation corresponds to an additional linear degeneracy, either in the Jacobian matrix for equilibrium points or in the Poincaré map for cycles.

When considering simultaneous variations of Q_1 and P_1 a double linear degeneration condition is detected. This condition corresponds to the double-zero or Bogdanov-Takens codimension-two bifurcation and the Jacobian (3.1) presents two eigenvalues at zero. The normal form of this bifurcation is given by

$$\begin{aligned}\dot{x} &= y + O(|x, y|^3), \\ \dot{y} &= \mu_1 + \mu_2 x + x^2 + sxy + O(|x, y|^3),\end{aligned}$$

where μ_1 and μ_2 are the main bifurcation parameters and $s = \pm 1$. The unfolding of this bifurcation for $s = 1$ is shown in Fig. 6 (the case $s = -1$ is very similar and can be seen in [14]). In region 1 there are no equilibria and crossing the curve SN1 towards region 2, two unstable equilibria are created due to a saddle-node bifurcation. Then the unstable node undergoes a subcritical Hopf bifurcation at the curve H^+ and becomes stable surrounded by an unstable limit cycle in region 3. This cycle is destroyed at the homoclinic bifurcation curve Hom. The stable node and unstable saddle equilibria of region 4 collapse at the saddle-node bifurcation curve SN2.

This singularity has been reported in [4] for the 3-bus model but for a different set of parameters. Notice that in [4] the Bogdanov-Takens bifurcation occurs for a negative value of P_1 . This point *a priori* seems to not have physical importance, but the emanating branches play a very important role in the system behavior for positive values of active power. In our investigation, the Bogdanov-Takens point is detected for positive values of P_1 (BT point at $Q_1 = 3.030710$ and $P_1 = 0.1524893$) but the bifurcation curves associated to the unfolding evolve toward negative values of P_1 as shown in Fig. 7.

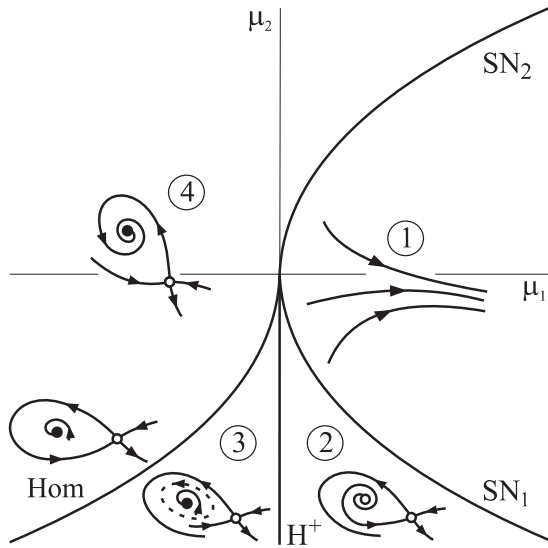


FIGURE 6. Unfolding of the Bogdanov-Takens bifurcation.

Let us describe in detail the bifurcation diagram of Fig. 7. The curves associated to the Bogdanov-Takens singularity are: the two branches of static saddle-node bifurcations (SN_1 and SN_2), the subcritical Hopf bifurcation (H^+) and the homoclinic bifurcation (Hom). These curves are shown in the expanded view of the rectangle of Fig. 7 and correspond to those predicted in the unfolding of Fig. 6. The curves $PD1$ and H^- are not directly related to this unfolding and deserve a particular description. The subcritical Hopf bifurcation curve emanating from the BT singularity becomes supercritical (H^-) at a generalized Hopf bifurcation. A cyclic fold curve arises at this codimension-two point (for simplicity it is not included in the diagram since it coalesces almost immediately with the homoclinic curve). It is important to mention that the generalized Hopf point occurs near the intersection of Hopf and homoclinic curves and the continuation task is very difficult to carry out in the neighborhood of this point. Nevertheless, partial numerical results seem to indicate that there exists a point on the homoclinic curve (Hom) where global complex phenomenon arises. This phenomenon requires the elements found around it: a homoclinic curve, a cyclic fold curve and a period doubling cascade. Thus, it could explain the collapse (or birth) of the period doubling bifurcation curve ($PD1$) on the homoclinic curve. Remember that $PD1$ is the first period doubling bifurcation in the cascade. Moreover, it could predict the collapse (or birth) of the period doubling cascade (see the mechanism in [18] and references therein). The analysis of this point is beyond the scope of this paper but, from a practical point of view, it is important since it is an organizing center of global dynamics that may affect operating regions. The dynamical phenomena displayed on Figs. 2 and 3 correspond to that obtained when varying Q_1 considering $P_1 = 0$, i.e. a

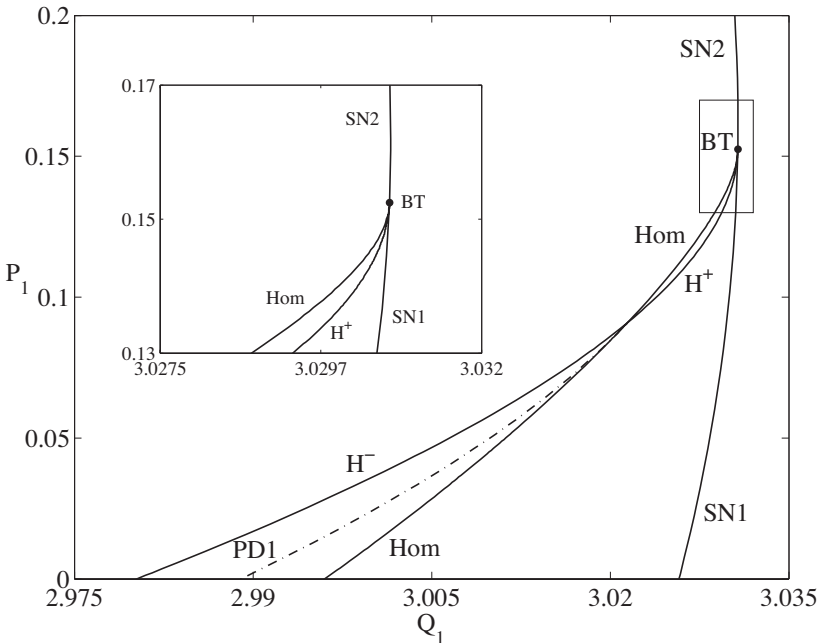


FIGURE 7. Two parameter bifurcation diagram.

horizontal cross-section at $P_1 = 0$ in Fig. 7. The period doubling curves associated to the cascade are not shown in this figure but they are located within the region enclosed by the locus of PD1 and that of Hom. Additional bifurcation phenomena on a larger region of the parameter plane, as well as vertical cross-sections (fixing Q_1 and varying P_1) can be consulted in [21].

5. CONCLUSIONS

In this paper an overview of representative one and two parameter bifurcation diagrams for a 3-bus power system model has been presented. The one parameter analysis has been performed varying the reactive power of the load Q_1 with the active power fixed at $P_1 = 0$. Saddle-node, Hopf and period doubling bifurcations have been detected. It has been shown that the cascade of period doubling bifurcations follows the Feigenbaum's theory and the value of Q_1 where the attractor exists has been predicted using Feigenbaum's constant. A two parameter bifurcation diagram has been obtained varying Q_1 and P_1 . A Bogdanov-Takens bifurcation for positive values of both parameters has been detected. In addition, evidence on the existence of an organizing center of global dynamics involving interactions between period doubling bifurcations and homoclinic orbits is discussed. Although the analyzed model is a simplified version of a real system, the mechanisms leading to voltage collapse can be used to alert against its occurrence in higher dimensional

models of power systems. The existence of global nonlinear phenomena restricting the basin of attraction of the operating point can also be expected.

REFERENCES

1. E. H. Abed and P. P. Varaiya, *Nonlinear oscillations in power systems*, Int. J. Electric Power and Energy Systems **6** (1984), no. 1, 37–43. [1](#)
2. P. M. Anderson and A. A. Fouad, *Power system control and stability*, IEEE PRESS Power System Engineering Series, New York, 1994. [1](#)
3. G. Andersson, P. Donalek, R. Farmer, N. Hatziargyriou, I. Kamwa, P. Kundur, N. Martins, J. Paserba, P. Pourbeik, J. Sanchez-Gasca, R. Schulz, A. Stankovic, C. Taylor, and V. Vittal, *Causes of the 2003 major grid blackouts in North America and Europe, and recommended means to improve system dynamic performance*, IEEE Trans. Power Systems **20** (2005), no. 4, 1922–1928. [1](#)
4. C. J. Budd and J. P. Wilson, *Bogdanov-Takens bifurcation points and Šil'nikov homoclinicity in a simple power-system model of voltage collapse*, IEEE Trans. Circuits Systems I **43** (2002), no. 5, 575–590. [1](#) [4](#)
5. I. Dobson and H. D. Chiang, *Towards a theory of voltage collapse in electric power systems*, Systems Control Lett. **13** (1989), no. 3, 253–262. [1](#) [2](#)
6. I. Dobson, T. Van Cutsem, C. Vournas, C. L. DeMarco, M. Venkatasubramanian, T. Overbye, and C. A. Cañizares, *Voltage stability assessment: Concepts, practices and tools*, ch. 2, IEEE Power Engineering Society, SP101PSS, August 2002. [1](#)
7. E. J. Doedel, R. C. Paffenroth, A. R. Champneys, T. F. Fairgrieve, Yu. A. Kuznetsov, B. E. Oldeman, B. Sandstede, and X.-J. Wang, *AUTO2000: Continuation and bifurcation software for ordinary differential equations (with HomCont)*, Tech. report, Caltech, California, 2002. [3](#)
8. M. J. Feigenbaum, *Qualitative universality for a class of nonlinear transformations*, J. Statist. Phys. **19** (1978), 25–52. [1](#) [3.1](#)
9. ———, *The universal metric properties of nonlinear transformations*, J. Statist. Phys. **21** (1979), 669–706. [1](#) [3.1](#)
10. J. Guckenheimer and P. Holmes, *Nonlinear oscillations, dynamical systems, and bifurcations of vector fields*, Springer Verlag, New York, 1993. [3](#)
11. D. J. Hill, Y. Guo, M. Larsson, and Y. Wang, *Global control of complex power systems*, Bifurcation Control (G. Chen, D. J. Hill, and X. Yu, eds.), Lecture Notes in Control and Information Sciences, vol. 293, Springer-Verlag, 2003, pp. 155–187. [1](#)
12. M. Ilić and J. Zaborszky, *Dynamics and control of large electric power systems*, John Wiley & Sons, Inc, New York, 2000. *
13. P. Kundur, *Power system stability and control*, McGraw-Hill, New York, 1994. [1](#)
14. Yu. A. Kuznetsov, *Elements of applied bifurcation theory*, Springer-Verlag, New York, 1995. [3](#), [†](#), [4](#)
15. H. G. Kwatny, A. K. Pasrija, and L. Y. Bahar, *Static bifurcations in electric power networks: loss of steady-state stability and voltage collapse*, IEEE Trans. Circuits Systems I **33** (1986), no. 10, 981–991. [1](#)
16. A. H. Nayfeh, A. M. Harb, and C. M. Chin, *Bifurcations in a power system model*, Int. J. of Bifurcation and Chaos **6** (1996), no. 3, 497–512. [1](#)
17. D. Novosel, M. M. Begovic, and V. Madani, *Shedding light on blackouts*, IEEE Power and Energy Magazine **2** (2004), no. 1, 32–43. [1](#)
18. B. E. Oldeman, B. Krauskopf, and A. R. Champneys, *Death of period-doublings: locating the homoclinic-doubling cascade*, Physica D **146** (2000), 100–120. [4](#)

19. M. A. Pai, P. W. Sauer, B. C. Lesieurte, and R. Adapa, *Structural stability in power systems-effect of load models*, IEEE Trans. Power Systems **10** (1995), no. 2, 609–615. [1](#)
20. L. Pereira, *Cascade to black*, IEEE Power and Energy Magazine **2** (2004), no. 3, 54–57. [1](#)
21. G. Revel, D. M. Alonso, and J. L. Moiola, *Bifurcation analysis in a power system model*, First IFAC Conf. on Analysis and Control of Chaotic Systems (Reims, France), 2006, pp. 315–320. [4](#)
22. W. D. Rosehart and C. A. Cañizares, *Elimination of algebraic constraints in power system studies*, IEEE Canadian Conf. on Electrical and Computer Engineering **2** (1998), 685–688. [*](#)
23. P. W. Sauer and M. A. Pai, *Power system dynamics and stability*, Prentice Hall, New Jersey, 1998. [1](#)
24. IEEE Power Engineering Society, *IEEE guide for synchronous generator modeling practices and applications in power system stability analyses*, IEEE Std 1110.-2002 (2003), 1–72. [2](#)
25. S. H. Strogatz, *Nonlinear dynamics and chaos*, Addison-Wesley, Reading, MA, 1994. [3.1](#)
26. C. W. Tan, M. Varghese, P. Varaiya, and F. F. Wu, *Bifurcation, chaos, and voltage collapse in power systems*, Proc. IEEE **83** (1995), no. 11, 1484–1496. [1](#)
27. C. D. Vournas, V. C. Nikolaidis, and A. A. Tassoulis, *Postmortem analysis and data validation in the wake of the 2004 Athens blackout*, IEEE Trans. Power Systems **21** (2006), no. 3, 1331–1339. [1](#)
28. K. Walve, *Modelling of power system components at severe disturbances*, International Conf. on Large High Voltage Electric Systems (CIGRÉ), 1986, pp. 1–9. [2](#)
29. H. O. Wang, E. H. Abed, and A. M. Hamdan, *Bifurcations, chaos, and crises in voltage collapse of a model power system*, IEEE Trans. Circuits Systems I **41** (1994), no. 3, 294–302. [1, 2, 3](#)

Gustavo Revel

Instituto de Investigaciones en Ingeniería Eléctrica (UNS-CONICET)
 Depto. de Ing. Eléctrica y de Computadoras,
 Universidad Nacional del Sur,
 Avda. Alem 1253, B8000CPB
 Bahía Blanca, Argentina.
grevel@uns.edu.ar

Diego M. Alonso

Instituto de Investigaciones en Ingeniería Eléctrica (UNS-CONICET)
 Depto. de Ing. Eléctrica y de Computadoras,
 Universidad Nacional del Sur,
 Avda. Alem 1253, B8000CPB
 Bahía Blanca, Argentina.
dalonso@criba.edu.ar

Jorge L. Moiola

Instituto de Investigaciones en Ingeniería Eléctrica (UNS-CONICET)
 Depto. de Ing. Eléctrica y de Computadoras,
 Universidad Nacional del Sur,
 Avda. Alem 1253, B8000CPB
 Bahía Blanca, Argentina.
jmoiola@criba.edu.ar

Recibido: 10 de abril de 2008

Aceptado: 18 de abril de 2008